ORIGINAL ARTICLE

Leaf protein allocation across the canopy and during senescence in earlier and later senescing maize hybrids, and implications for the use of chlorophyll as a proxy of leaf N

Mariana Antonietta[1] · Paula Girón[1,2] · María L. Costa[1] · Juan J. Guiamét[1]

Abstract

Leaf chlorophyll (chl) and protein distribution were analyzed throughout grain filling in four modern maize hybrids with contrasting senescence behavior, at three different canopy levels and at low-N (LN, 18 kg N ha^{-1}) and high-N (HN, 218 kg N ha^{-1}) fertilization levels. Chl content assessed by SPAD resembled protein content only at LN, with delayed senescing genotypes having more leaf protein content than reference genotypes. Across N levels, relative chl content negatively related to light intensity ($r^2 = 0.59$, $P < 0.001$), while relative protein content did only for the lowest part of the canopy ($r^2 = 0.54$, $P < 0.001$), suggesting protein distribution in the canopy could be further improved. Relative Rubisco/LHCII partitioning increased from lower to upper leaves ($P < 0.09$) and differed among genotypes ($P < 0.05$) with no link to senescence behavior. Photosynthetic electron transport rates were lower at LN and differed between genotypes ($P < 0.05$) including those with similar leaf protein contents. Chl and protein contents were related across the entire dataset ($r^2 = 0.53$, $P < 0.001$) but the slope (b) of this relationship varied widely depending on the leaf position ($b = 0.026–0.019$), the senescence stage ($b = 0.014–0.020$), the N level ($b = 0.035–0.026$) and the hybrid ($b = 0.016–0.033$). Our results suggest that in modern maize hybrids, leaf N utilization can be further improved and that genotypic together with other sources of variation should be included as specific variables in SPAD-based predictions of leaf N content.

Keywords Nitrogen · Stay green · Leaf · Senescence · Protein · *Zea mays*

Introduction

Worldwide, the increasing cost of N fertilizers emphasizes the importance of improving N use efficiency (grain yield/soil N, NUE). In Argentinean maize crops, fertilizers can account for ca. 35% of total input costs whereas urea is the main expenditure after the seeds (Cabrini et al. 2017). Genotypic variability for yield under low-N environments may relate to differences in N utilization efficiency (NUtE, grain yield/N uptake) since, when soil N is scarce, N uptake efficiency (N uptake/soil N) becomes higher and comparatively less yield determinant (Gallais and Coque 2005). In this line, post-silking N uptake can be less than 20% of total plant N at harvest (e.g., Cirilo et al. 2009; Chen et al. 2015; Antonietta et al. 2016) whereas regarding pre-silking N, the relative contribution of leaf N to stover N remobilization may account for up to 62% (Kosgey et al. 2013; Chen et al. 2015). Genotypic variation for NUtE at the leaf level is evidenced in modern maize hybrids presenting similar post-silking N uptake but differing for rates of canopy senescence and leaf N content at harvest (Kosgey et al. 2013; Acciaresi et al. 2014; Antonietta et al. 2014, 2016). Further, Chen et al. (2014) found genotypes achieving similar yield and senescence rates while differing for N remobilization efficiency, N photosynthetic use efficiency and grain N concentration, highlighting targets to improve NUtE.

✉ Mariana Antonietta
antoniettamariana@gmail.com

1 Instituto de Fisiología Vegetal (INFIVE), Universidad Nacional de La Plata-CONICET, cc 327, La Plata, CP 1900, Buenos Aires, Argentina

2 Present Address: EEA General Villegas, INTA, San Martín No. 26, 6230 General Villegas, Argentina

In the canopy, maize leaves are exposed to light intensities that span from 90% of incident light in the upper part of the canopy to less than 10% in middle- to low-positioned leaves (Acciaresi et al. 2014). This determines a N gradient (higher protein concentration in upper leaves) that improves N photosynthetic efficiency at the plant level (Gastal and Lemaire 2002; Chen et al. 2016). NUtE is also improved by changes in relative protein abundance (increased proportion of proteins involved in light harvesting towards the base of the canopy, e.g., Evans and Poorter 2001) and by metabolic changes including reduced respiration losses and leakiness in lower leaves (Bellasio and Griffiths 2014).

Overall, under low N conditions, NUE at the leaf level is improved across the canopy, being higher in upper leaves (Chen et al. 2016). All this environmental as well as genotypic modulation of N use at the leaf level imply a bias in chl-based leaf N estimations (Xiong et al. 2015) which are widely used in plant physiology, as well as in regional-scale analyses (NVDI) and for agronomic purposes.

There are several works on NUtE at the leaf level comparing N doses (Mu et al. 2016), hybrids (Chen et al. 2014) and leaf positions (Chen et al. 2016), but, as far as we know, there are not works including comparisons that combine contrasting N levels, hybrids, leaf positions and senescence stages. We hypothesize that there is genotypic variability for N use at the leaf level, and that this variation is partially related to canopy senescence behavior. The main objective of this work was to analyze genotypic variability for the pattern of protein–N distribution within leaves in different positions in the canopy, and its changes during senescence. The specific objectives of this work were to describe, for four modern maize hybrids with contrasting senescence behavior and for three leaves at different positions in the canopy under two N inputs, (1) chl and (2) protein content through senescence stages, (3) light modulation of chl and protein contents, (4) the ratio between different chloroplastic protein fractions (Rubisco and LHCII), (5) photosynthetic electron transport rates (ETR) and finally, (6) implications for chl vs. protein correlations.

Materials and methods

Experimental design

A field experiment was conducted in 2010–2011 at the Experimental Field of Facultad de Ciencias Agrarias y Forestales (Universidad Nacional de La Plata) (34°54′24″S; 57°55′56″W, Argentina). Treatments consisted of two N fertilization levels and four modern, commercial maize hybrids, and were arranged in a split-plot design with three blocks (replicates). N level was randomized in the main plots while hybrids were randomized in each subplot. Subplots consisted of four rows, 0.7 m apart and 7 m long ($19.6 m^2$). At sowing, all the treatments received 18 kg N ha^{-1} applied as diammonium phosphate. In the low-N treatment (hereafter, LN) no extra N was applied while the high-N treatment (HN) was achieved by fertilizing with 200 kg N ha^{-1} applied as urea in two equal doses at V3 and V6 stages (the third and sixth leaf with visible ligules, respectively, Ritchie et al. 1996). These N fertilization levels aimed at generating contrasting plant performances, with (LN) and without (HN) N limitations since previous works showed a lack of yield response to N doses higher than 200 kg ha^{-1} (e.g., Chen et al. 2016). Also, under the conditions of the experiment reported here, grain yield response was mostly saturated at 100–200 kg N Ha^{-1} (Antonietta et al. 2016). The soil was a typical argiudoll (USDA classification) with a fine texture and an underlying layer (40 cm deep) of expandable clay. Total soil N was 0.16% between 0 and 20 cm, 0.13% between 20 and 40 cm and 0.10% between 40 and 60 cm. Further details on crop management can be found in Antonietta et al. (2016).

In the subplots, four hybrids previously characterized by having contrasting senescence behavior but similar days to silking and similar cycle length (Antonietta et al. 2014) were sown. The DK682 and AW190 hybrids have an early-senescing behavior (non-stay green, hereafter, NSG), while the AX878 and NK880 hybrids show a functional delay in senescence (stay green, hereafter, SG).

Seeds were sown manually on 12 November 2010, and seedlings were thinned to a final plant density of 8 pl m^{-2}. Silking occurred around 80 days after sowing and differences in silking date between N treatments or hybrids were of 3 days at most. Plots were irrigated as needed from emergence to maturity to prevent water deficit and were maintained free of weeds by the application of herbicides when needed.

Sampling procedure

In each treatment, three leaves representing different canopy positions were sampled: the third leaf below the ear (hereafter, leaf − 3), the ear leaf (leaf 0) and the third leaf above the ear (leaf + 3). For each N dose and leaf position, three samplings were made. The first sampling was made at around silking for all N × leaf combinations. The second and third sampling dates took place when the SPAD value of the NSG hybrid, DK682 (which was taken as a reference), had decreased by at least 20% and 40%, respectively, of the value achieved at silking in each N x leaf combination. In each sampling date, three replicates were taken, each consisting of a compound sample of leaves obtained from two plants.

Chl measurements

On each sampling date, leaves were cut from the plant between 9 and 11 am and stored in an icebox in darkness and with a saturated water vapor atmosphere for no more than 2 h. In these leaves, chl content was assessed by SPAD measurements (Minolta SPAD 502). The SPAD value recorded in each leaf corresponded to the average of five measurements taken in the middle third of the leaf lamina and in a central position between the midrib and the leaf margin.

Protein determinations

In the same leaf sections where SPAD measurements were made, leaf discs (1 cm diameter) were punched, frozen in liquid N_2 and stored at -20 °C for protein determination. Leaf extracts were made according to Kingston-Smith and Foyer (2000) with some changes, allowing for the extraction of water-soluble and detergent-soluble proteins and detergent-soluble proteins. Leaf extracts were made by homogenizing three leaf discs (a total leaf area of 2.36 cm^2) with 200 µL extraction buffer (Tris–HCl 125 mM, pH 7.8, 0.1% v/v of Triton X-100, 5 mM $MgCl_2$, 5 mM cysteine, 1 mM PMSF and 10 µM leupeptin). The homogenate was vortexed for 60 s, sonicated for 280 s, placed at 60 °C for 10 min and centrifuged at 9000g (5 min).

Protein determination was made by SDS-PAGE. Polyacrylamide gels were prepared according to Laemmli (1970), using gels of 10% polyacrylamide and 1.5 mm thickness. Equal amounts of sample (35 µL extract, equivalent to a leaf area of 0.4 cm^2) were loaded in each lane. In each gel, a single replicate including the three leaves and three senescence stages of each N dose × hybrid combination was loaded (nine samples per gel). In addition, three lanes with different amounts of a reference protein (bovine serum albumin) were loaded as a standard. Gels were run at 12 mA per gel for 2.5 h and then stained in a Coomassie blue solution for at least 1 h and finally distained.

Protein quantification was made by scanning the gels to obtain digital images. To determine the protein content in the samples, the SIGMA-Gel software was used. The protein bands were quantified by comparison to a calibration curve obtained from the three lanes with reference protein loaded in each gel.

Protein blotting and quantitation of Rubisco and LHCII

For protein blotting, proteins were electro-transferred to nitrocellulose membranes at 100 mA for 1.5 h. Blots were blocked overnight at 4 °C with 5% (w:v) non-fat dry milk dissolved in TBS-T (20 mM Tris, pH 7.4, 150 mM NaCl, 0.02% [v:v] Tween-20). Next, blots were incubated overnight at 4 °C in primary antibody dissolved in blocking buffer, and then washed five times (10 min each) with TBS-T. Blots were then incubated for 1 h in secondary antibody (goat anti-rabbit IgG conjugated to horseradish peroxidase), washed several times with TBS-T and developed with a chemiluminescence detection kit. For Rubisco and LHCII detection, polyclonal rabbit antibodies were used as primary antibody. The Rubisco antibody was raised at INFIVE against purified Swiss chard Rubisco while the LHCII antibody was donated by Dr. O. Vallon (French National Center for Scientific Research, Paris, France).

Light transmittance

Light transmittance was determined at around silking, during midday on a sunny day with an AccuPAR linear (1 m long) light meter (Decagon, WA, USA). The line sensor was placed diagonally covering all the distance between two adjacent rows at four different heights corresponding to the nodes of leaf $+3$, leaf 0, leaf -3 and leaf -7 (i.e., total light interception).

Photosynthetic electron transport rate measurements

Photosynthesis was estimated from chl fluorescence measurements (ETR). A pulse-amplitude-modulated FMS2 (Hansatech, UK) chl fluorometer was used to measure the effective PSII quantum yield. Measurements were taken at midday, on fully illuminated spots of the ear leaf of eight plants per treatment (two plants per subplot). In the same spot where ETR measurements were performed, the SPAD value was recorded. ETR was calculated as in Rosenqvist and van Kooten (2003), except that leaf absorptance was corrected by the SPAD value of each individual leaf, as in Acciaresi et al. (2014):

$$ETR = PAR \times Abs \times \phi PSII \times 0.5,$$

where PAR is photosynthetically active radiation, Abs is leaf absorptance ($= 0.008 \times SPAD + 0.356$), and ϕPSII is effective photosystem II quantum yield. In C_4 plants, ETR measurements correlate closely with photosynthetic rates (Earl and Tollenaar 1999).

Statistical analysis

Data were analyzed with the STATISTICA 5.1 software (StatSoft, Inc.), using ANOVA for the detection of statistical differences between factors and their interactions.

Each N level × leaf combination was analyzed separately. For each N level × leaf combination, "hybrid", "sampling date" and "replicate" were analyzed as fixed factors. Comparisons involving different N levels or leaves were made

only with data obtained at silking, using "N level", "leaf" and "hybrid" as fixed factors. When factors or their interactions were significant, means were compared by the LSD test ($P < 0.05$). For linear regressions, the significance was assessed through the F test ($P < 0.05$).

Results

Leaf senescence

At silking and at all leaf positions, hybrids had lower SPAD values in LN (Fig. 1a–c) compared with HN (Fig. 1d–f). Both SGs NK880 and AX878 achieved higher SPAD values than the intermediate AW190 and the NSG DK682 (except for leaf − 3 in AX878 at HN), this difference being more conspicuous at LN. Across the crop cycle, and consistently for all leaf positions, NK880 was the slowest senescing (circle symbols above the rest at the last sampling, Fig. 1a–f), except for leaf − 3 under HN. By contrast, the senescent behavior for AX878 could not be distinguished from a NSG type such as AW190 in some leaves (leaf − 3 at LN, Fig. 1a, leaf 0 and + 3 at HN, Fig. 1e, f; Supp. Table 1).

Protein content

At silking and for all leaf positions, protein content in LN was 50–60% lower and decreased during senescence at a faster rate (Fig. 2a–c) compared with HN (Fig. 2d–f). At LN, both SG hybrids showed higher protein contents than AW190 and DK682 throughout senescence (Fig. 2a–c, Supp. Table 1). In HN, hybrid's behavior followed a different trend from that observed at LN since the highest protein contents were found only in the SG AX878, while the SG NK880 could not be distinguished from AW190 and DK682 on the basis of protein contents across the crop cycle (Fig. 2d–f, Supp. Table 1). In addition, while at LN leaf protein contents resembled the trend observed for chl decline, this did not hold for HN since the SG NK880, with the lower rates of chl decline, could not be distinguished from a NSG type on the basis of their leaf protein contents.

Light transmittance across the canopy and chl and protein gradients

Light transmittance decreased across the canopy and overall, the SG hybrid AX878 showed a lower flux of light reaching to leaves at upper and middle positions (Supp. Figure 1).
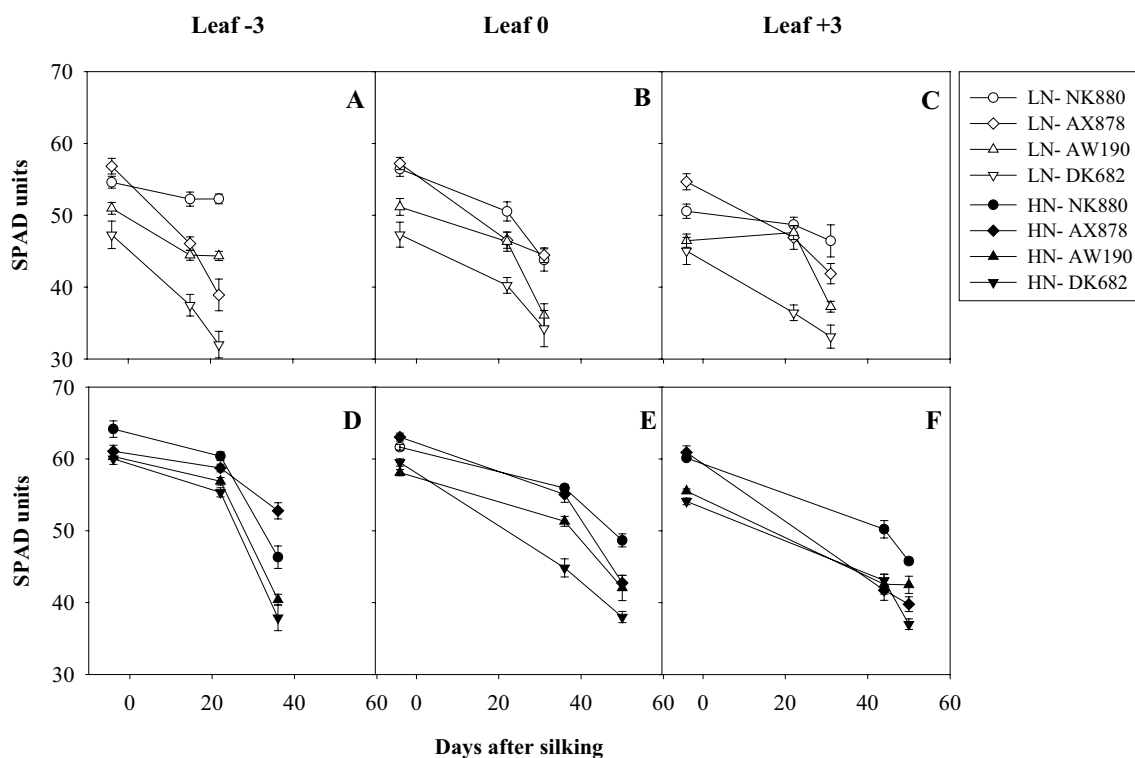

Fig. 1 Leaf chlorophyll content (SPAD units) throughout senescence. Separate panels are shown for LN (18 kg N ha^{-1}, **a–c**) and HN (218 kg N ha^{-1}, **d–f**), and leaf position: third leaf below the ear (**a**, **d**), ear leaf (**b**, **e**) and third leaf above the ear (**c**, **f**). Different symbols represent maize hybrids: circles, NK880; diamonds, AX878; upward triangles, AW190; downward triangles, DK682. Lines over the symbols indicate the standard error
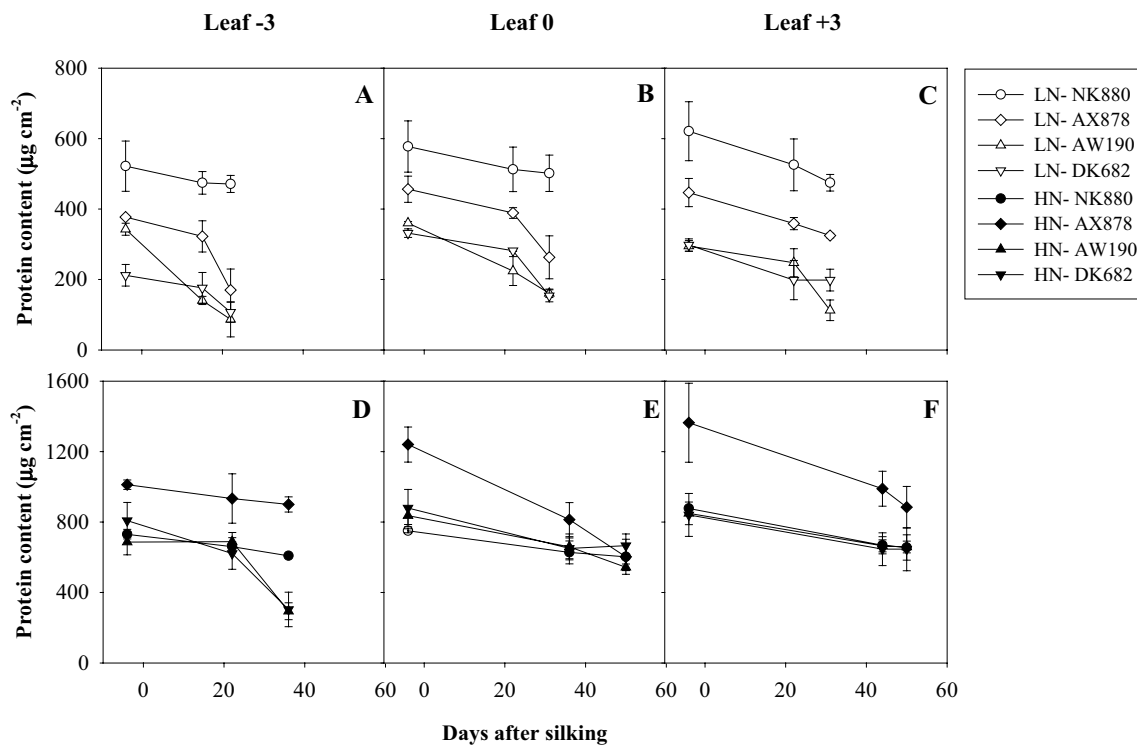
Fig. 2 Leaf protein contents ($\mu g\ cm^{-2}$) throughout senescence. Separate panels are shown for LN (18 kg N ha^{-1}, **a–c**) and HN (218 kg N ha^{-1}, **d–f**), and leaf position: third leaf below the ear (**a**, **d**), ear leaf (**b**, **e**) and third leaf above the ear (**c**, **f**). Different symbols represent maize hybrids: circles, NK880; diamonds, AX878; upward triangles, AW190; downward triangles, DK682. Lines over the symbols indicate the standard error. Note different scales in the "Y" axis for LN and HN

As expected, relative chl distribution in the canopy negatively related to light intensity ($r^2 = 0.59$, $P < 0.001$, Fig. 3a). By contrast, relative protein distribution related positively to light intensity only below 40% of light transmittance ($r^2 = 0.54$, $P < 0.001$, Fig. 3b). At a higher light intensity, relative protein content in the leaves was similar or even
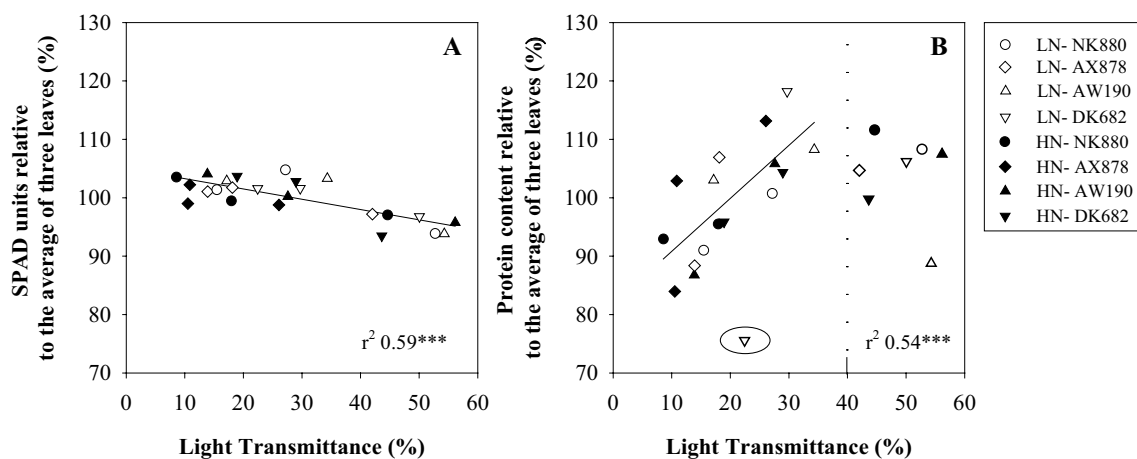

Fig. 3 Correlation between percentages of photosynthetic photon flux density (% PPFD) transmitted across the canopy and SPAD units (**a**) or leaf protein content (**b**) across N levels. SPAD and protein contents were expressed as a percentage of the average of the three leaf positions in each hybrid. Each point is the average of three replicates.

Symbols denote the treatment: empty symbols, LN; full symbols, HN; circles, NK880; diamonds, AX878; upward triangles, AW190; downward triangles, DK682. In **b**, points beyond the dashed line were not considered in the regression

lower than the one achieved under lower irradiances evidencing a non-optimum distribution of leaf protein across the canopy.

Relative contents of different protein fractions

The relative content of different protein fractions was analyzed at HN (Supp. Figure 2, Fig. 4). The proteins analyzed, Rubisco and LHCII, differ in their location in the chloroplast: Rubisco is a soluble protein key in C fixation accounting for 33% of the leaf-N engaged in soluble proteins (Makino et al. 2003). By contrast, LHCII strongly binds to the thylakoid membrane and is involved in light harvesting, representing around 15% of leaf-N engaged in insoluble proteins (Makino et al. 2003). At silking, the Rubisco/LHCII ratio averaged across hybrids was higher ($P < 0.09$) in the more illuminated, leaf $+ 3$ (1.02) than in either leaf 0 (0.87) or leaf $- 3$ (0.77). Significant hybrid

differences were detected in leaf 0 and leaf $+ 3$, the SG AX878 and the NSG AW190 having higher Rubisco/LHCII ratios than the SG NK880 and the NSG DK682 (Fig. 4b, c).

Photosynthetic electron transport rate

Chl fluorescence was measured in the ear leaf at mid-grain filling (31 DAS), during midday and at full irradiance, to estimate photosynthetic electron transport rate (ETR). In LN, ETR was higher in the SG hybrid NK880 and no differences were found within the rest of the hybrids (Fig. 5) in spite of their different protein contents (compare DK682 with AX878 or AW190, Fig. 2b). In HN, no hybrid differences were detected. Light on the leaf spot where ETR determinations were taken did not differ among hybrids (data not shown).
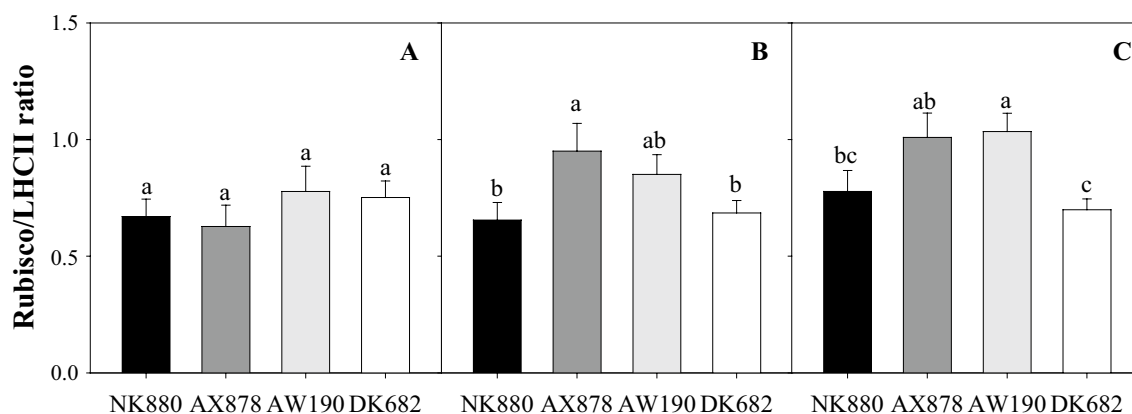

Fig. 4 Relative Rubisco and LHCII contents at HN in the third leaf below the ear (**a**), the ear leaf (**b**) and the third leaf above the ear (**c**). The bar color denotes the hybrid: black, NK880; dark gray, AX878; light gray, AW190; white, DK682. No significant interaction was detected for hybrid × sampling date, thus data are averages of three sampling dates starting at silking. Lines above the bars show the standard error of the mean while letters show homogenous groups for LSD ($P < 0.05$)

Fig. 5 Electron transport rate (ETR) at 31 days after silking at low (LN) and high N level (HN). Each bar is the average of eight independent measurements taken around midday in fully illuminated spots of the ear leaf. The bar color denotes the hybrid: black, NK880; dark gray, AX878; light gray, AW190; white, DK682. Lines above the bars show the standard error of the mean while letters show homogenous groups for LSD ($P < 0.05$)
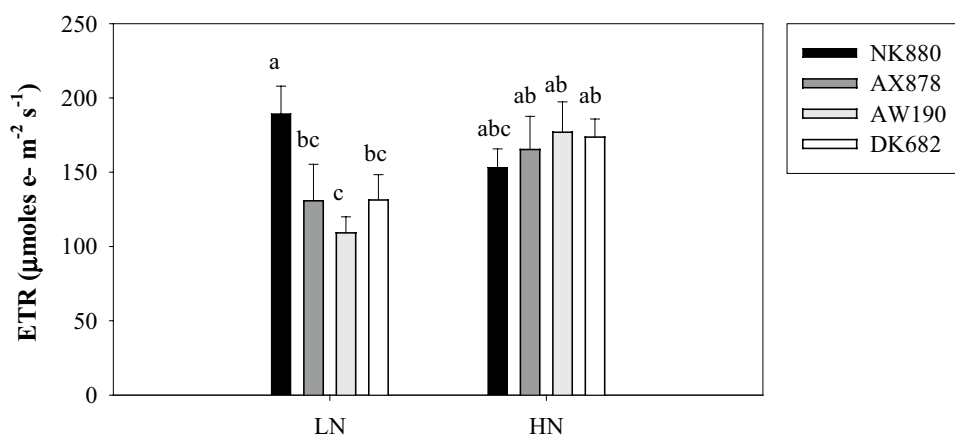
Protein vs. Chl correlations

In view of the wide use of chl as a proxy of leaf N content, we analyzed the implications of leaf, senescence stage, N level and genotypic variability over SPAD vs. protein correlations. While most of the relationships were significant according to $P < 0.001$, important variation in slopes (b) was observed. By plotting all the data together, we obtained a significant relationship ($r^2 = 0.53$, $b = 0.022$) though considerable scattering was observed in some data ranges (e.g. > 20 units of SPAD variation at protein contents ca. 600 µg cm^{-2},
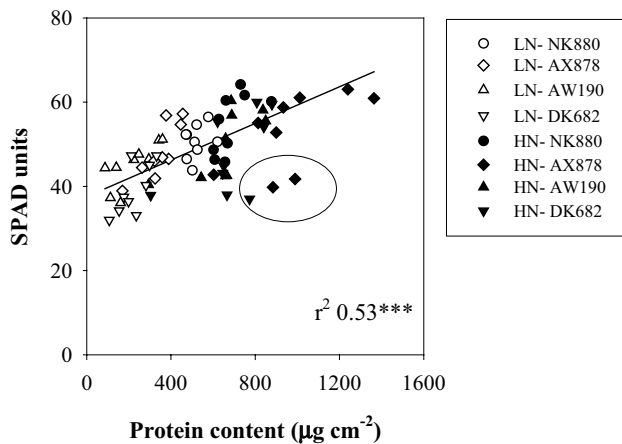

Fig. 6 Regression analyses between leaf protein contents and SPAD units across the entire dataset (2 N levels × 4 hybrids × 3 leaves × 3 senescent stages). Each point is the average of three replicates. Symbols denote the treatment: empty symbols, LN; full symbols, HN; circles, NK880; diamonds, AX878; upward triangles, AW190; downward triangles, DK682. The encircled points were not included in the regression. Parameters obtained from the fitted linear equations are $y = 0.022x + 38$. ***$P < 0.001$
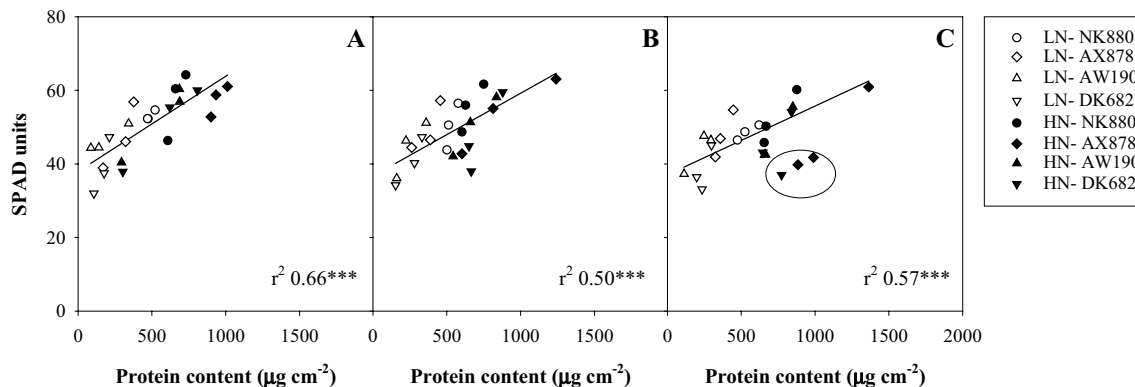
Fig. 6). When the source of variation was the leaf position, the r^2 coefficient and slope were higher for leaf -3 (Fig. 7a, $r^2 = 0.66$ and $b = 0.026$) than for leaves 0 (Fig. 7b, $r^2 = 0.50$ and $b = 0.022$) or $+3$ (Fig. 7c, $r^2 = 0.57$ and $b = 0.019$). During the grain filling, the relationship was closer for leaves at silking but with a lower slope (Fig. 8a, $r^2 = 0.59$ and $b = 0.014$) than for senescing leaves (Fig. 8b, $r^2 = 0.47$ and $b = 0.020$). Analyzing separately each N level, a linear fit was obtained at LN (Supp. Figure 3A, $r^2 = 0.55$) while a polynomial adjustment was better for HN indicating a loss of correlation at protein contents higher than ca. 700 µg protein cm^{-2} (Supp. Figure 3B, $r^2 = 0.51$). Regarding genotypes, protein content varied very little in the SG NK880 (Supp. Figure 4A); in the rest of the hybrids, a greater range of variation for protein content allowed more meaningful comparisons to be made. The slope was lowest for the SG AX878 (Supp. Figure 4B, $r^2 = 0.60$ and $b = 0.016$), intermediate for AW190 (Supp. Figure 4C, $r^2 = 0.42$ and $b = 0.026$) and highest for the NSG DK682 (Supp. Figure 4D, $r^2 = 0.61$ and $b = 0.033$).

Discussion

At around silking, leaves account for as much as 66% of total plant N (Kosgey et al. 2013), which is mainly located in photosynthetic proteins (Gastal and Lemaire 2002). Under N deficiency, the reduction in leaf protein content (e.g., by 53% in the present work) implied a concomitant reduction in the amount of remobilizable N for developing grains (Masclaux-Daubresse et al. 2010). This may be partially offset by an increase in relative leaf protein degradation, especially in lower leaves which senesce earlier (e.g., Acciaresi et al. 2014). In this line, the total amount of remobilized N was

Fig. 7 Regression analyses between leaf protein contents and SPAD units for the third leaf below the ear (**a**), the ear leaf (**b**), and the third leaf above the ear (**c**). Each point is the average of three replicates. Symbols denote the treatment: empty symbols, LN; full symbols, HN; circles, NK880; diamonds, AX878; upward triangles, AW190; downward triangles, DK682. The encircled points were not included in the regression. Parameters obtained from the fitted linear equations are **a** $y = 0.026x + 38$; **b** $y = 0.022x + 37$; **c** $y = 0.019x + 37$. ***$P < 0.001$
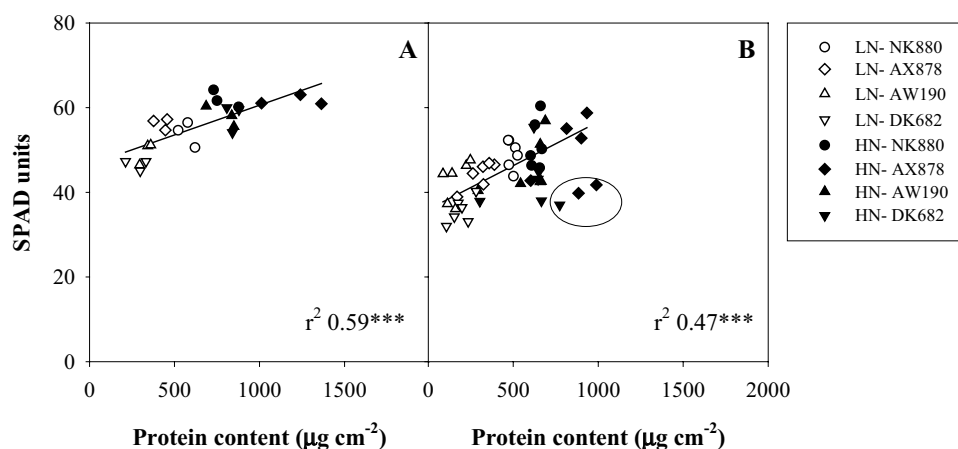
Fig. 8 Regression analyses between leaf protein contents and SPAD units for leaves sampled at silking (**a** $n = 24$) and for leaves sampled 15 days after silking and thereafter (**b** $n = 48$). Each point is the average of three replicates. Symbols denote the treatment: empty symbols, LN; full symbols, HN; circles, NK880; diamonds, AX878; upward triangles, AW190; downward triangles, DK682. The encircled points were not included in the regression. Parameters obtained from the fitted linear equations are **a** $y = 0.014\ x + 46$; **b** $y = 0.020\ x + 36$. ***$P < 0.001$

reduced by 30%, while the % leaf N at harvest was reduced by 45% under LN (Antonietta et al. 2016).

Across the canopy, leaf ontogeny (and the co-occurrence of specific ontogenic leaf stages with grain N demand) may have an important role in determining the relative contribution of each leaf to total grain N. It is known that N content in leaves at harvest decreases and N remobilization increases from upper to lower leaves (He et al. 2002, results in the present paper), with lower leaves senescing earlier and close to key stages of grain development (e.g., Below et al. 2000).

In this work, protein decrease relative to the content achieved at silking was higher in leaf − 3 or leaf 0 compared with leaf + 3 in all hybrids (60, 50 and 36%, respectively, calculated from data in Fig. 2) except for the SG NK880 (15, 7 and 21% for leaf − 3, 0 and + 3, respectively). This suggests that in some cases, leaf senescence may not respond closely to N demand by sinks. A possible explanation is supported by the "senescence window concept" (Schippers et al. 2015): the environmental and timing requirements for achieving competence to senesce may be genotype dependent.

Moreover, the relative senescence behavior of the hybrids depended on leaf position (e.g., AX878 showed an early-senescent behavior in the lower leaf, Fig. 1a) as shown previously (Paponov et al. 2005; Antonietta et al. 2014), suggesting that (1) the activity of the senescence regulating factors may vary throughout the plant in a genotype-dependent fashion, and/or (2) senescence proceeds independently at different canopy positions. Exploiting non-simultaneous senescence behavior of different leaf layers may improve the role of lower leaves as N source while maintaining enough C assimilation by upper leaves. In fact, relative yield reduction between LN and HN was lowest for AX878 (12%) and highest for AW190 and NK880 (22%) (Antonietta et al. 2016) which is in line with the way N was utilized at the leaf level: AX878 achieved almost similar leaf protein contents as NK880 but it was able to remobilize this N efficiently reaching the same values as its NSG counterparts by 31 DAS, especially in leaves − 3 and 0 (Fig. 2a, b) exposed to less than 15% of the light intensity reaching the top of the canopy (Supp. Figure 1A). In line with this, Acciaresi et al. (2014) showed that N content in basal canopy leaves of a SG hybrid was much higher than the minimum needed to exploit the low light intensity these leaves were exposed to.

In maize, around 42% of leaf N is located in the chloroplast distributed between membrane proteins mainly involved in light capture reactions, such as LHCII and soluble proteins implicated in CO_2 assimilation, such as Rubisco (Makino et al. 2003). A lower investment in Rubisco and/or a delay in LHCII degradation (Hidema et al. 1991) in leaves growing under low irradiances improves N utilization and is evident in the present work as a lower Rubisco/LHCII ratio in leaf − 3 (Fig. 4). No apparent association was found between the Rubisco/LHCII ratio and chl retention, which contrasts with previous works reporting higher N partitioning to Rubisco in a senescent hybrid compared with a SG one (He et al. 2002) and suggest that N partitioning inside the leaf is relatively independent of the senescence behavior.

In C4 species, photosynthetic electron transport rate (ETR) is linearly related to photosynthesis, i.e., CO_2 assimilation (Earl and Tollenaar 1999), which, in turn, relates to leaf protein content. In maize, photosynthetic rates are reported to decrease when leaf N content drops below 1.75–1.5 g N m^{-2} (Makino et al. 2003; Paponov et al. 2005). Here, at LN, higher ETR was achieved by NK880 (Fig. 5a) which may relate to its higher protein content (Fig. 2b).

For the rest of the hybrids, the lack of differences for ETR together with differences in protein content suggests higher photosynthetic efficiency per unit N (PNUE) in the early-senescing DK682. Similarly, He et al. (2002) report higher PNUE in an early-senescing hybrid compared with a late-senescing one. Higher PNUE under LN has been related to an increase in N partitioning to proteins involved in electron transport and photophosphorylation (including Cyt b/f and CF_1/CF_0) (Mu et al. 2016) and may explain, in part, differences for PNUE among hybrids.

While there is ample evidence that a non-uniform N distribution across the canopy enhances C assimilation (Gastal and Lemaire 2002), photosynthetic N use efficiency could still be improved since it is lower in low-positioned leaves compared with upper ones (Acciaresi et al. 2014; Chen et al. 2016). Our results show that the protein gradient across the canopy, with leaf protein content increasing as irradiance increases, is lost above 40% of light transmittance (Fig. 3b) in all the hybrids and at both N levels (except for AX878 under HN). This suggests that the already-reported above-optimum N content in low-canopy leaves may occur simultaneously with below-optimum N content in upper leaves. Improving processes that modulate protein distribution according to the light environment may increase the NUtE at the canopy level. By contrast, chl represents a very small part of total leaf N (ca. 1.3%, calculated from Xiong et al. 2015), and this may be the reason why the development of a chl gradient in response to irradiance may be easier to achieve, and not affected by N level or genotype (Fig. 3a).

At the leaf level, N is mostly located in the chloroplast (43% of leaf N), particularly in thylakoid-membrane proteins (Makino et al. 2003). Much less is located in chl, which represents only around 1.3% of total leaf N (calculated from Xiong et al. 2015). Nonetheless, the development of optical techniques which allow non-destructive and fast measurement of chl content in leaves, such as SPAD and "green seekers", has led to the wide use of chl as a senescence biomarker in different species including maize (e.g., Osaki 1995). Furthermore, many authors encourage the use of chl as a proxy of leaf N content (e.g., van Oosterom et al. 2010) and many companies promote "green seekers" as tools for N management in crops (e.g., Trimble). The results presented here indicate that in many situations, chl may lead to misprediction of leaf N.

Because chl:protein relations are reported to be closer for membrane proteins than for soluble or total leaf proteins (Thomas et al. 2002), the higher proportion of thylakoid-associated proteins such as LHCII in lower positioned leaves may explain the better adjustment and higher slope of chl:protein relations found in this leaf (Fig. 7). This could be a concern since upper leaves presumably contribute a large part of the reflectance signal received by some sensors. On the other hand, we found a progressive loss of adjustment in chl vs. protein regressions as senescence developed (Fig. 8), suggesting that environmental or genotypic modulation of chl vs. protein relations is more pronounced during senescence than during earlier leaf development. Little is known about the contribution of proteins located outside the chloroplast to total leaf N of senescing leaves, which, before senescence, may account for at least 38.7% of total leaf N (Makino et al. 2003). At high N level, excess N may be stored in leaves as protein (mainly Rubisco) without a concomitant increase in chl (Hirel et al. 2005), and the relative contribution of soluble protein to total leaf protein may increase (Mu et al. 2016), both leading to a loss of adjustment of chl vs. protein relations (Supp. Figure 3). Finally, the slope of chl–protein regressions was increasingly higher from the SG AX878 to AW190 and DK682, the NSG reference (Supp. Figure 4). Such a behavior indicates a faster rate of chl loss per unit of N loss (due to senescence, N input or leaf position) in early-senescing hybrids (He et al. 2002), which probably is due to membrane proteins since genotype-specific curvilinear relations between leaf N and chl content are not due to differences in soluble proteins (Hirel et al. 2005).

Conclusion

The results of this paper show genotypic variation for protein–N distribution within different leaves in the canopy and throughout senescence. Delayed senescence genotypes appear to have initially higher leaf protein contents under LN, but not necessarily under HN, suggesting that increased leaf N content may be a requirement for delaying senescence under LN. Other findings suggest targets to further improve NUtE. (1) The development of a N gradient across the canopy is lost above 40% light transmittances independently of the N input or the genotype, showing a possibly lower than optimum N content in upper leaves. (2) Rubisco/LHCII partitioning varies between hybrids without association with the light profile or the senescence behavior. (3) Similar ETR are achieved with different leaf protein contents. Finally, variation in N partitioning across canopy leaves, during senescence and between N environments and genotypes results in variability for chl vs. protein regressions which should be considered when using chl-based measurement as a proxy of leaf N content.

Compliance with ethical standards

Conflict of interest The authors declare no conflicts of interest.

References

Acciaresi HA, Tambussi EA, Antonietta M, Zuluaga MS, Andrade FH, Guiamet JJ (2014) Carbon assimilation, leaf area dynamics, and grain yield in contemporary earlier and later-senescing maize hybrids. Eur J Agron 59:29–38

Antonietta M, Fanello DD, Acciaresi HA, Guiamet JJ (2014) Senescence and yield responses to plant density in stay green and earlier-senescing maize hybrids from Argentina. Field Crops Res 155:111–119

Antonietta M, Acciaresi HA, Guiamet JJ (2016) Responses to N deficiency in stay green and non stay green Argentinean hybrids of maize. J Agron Crop Sci 202:231–242

Bellasio C, Griffiths H (2014) Acclimation of C4 metabolism to low light in mature maize leaves could limit energetic losses during progressive shading in a crop canopy. J Exp Bot 65:3725–3736

Below F, Cazetta J, Seebauer J (2000) Carbon/nitrogen interactions during ear and kernel development of maize. In: Physiology and modeling kernel set in maize. Crop Science Society of America and American Society of Agronomy. Special publication number 29

Cabrini SM, Llovet JA, Bitar MV, Paollili MC (2017) Márgenes brutos de las principales actividades agrícolas. Campaña 2017/2018. INTA Pergamino. https://inta.gob.ar/sites/default/files

Chen Y, Xiao C, Chen X, Li Q, Zhang J, Chen F, Yuan L, Mi G (2014) Characterization of the plant traits contributed to high grain yield and high grain nitrogen concentration in maize. Field Crops Res 159:1–9

Chen Y, Xiao C, Wu D, Xia T, Chen Q, Chen F, Yuan L, Mi G (2015) Effects of nitrogen application rate on grain yield and grain nitrogen concentration in two maize hybrids with contrasting nitrogen remobilization efficiency. Eur J Agron 62:79–89

Chen Y, Wu D, Mu X, Xiao C, Chen F, Yuan L, Mi G (2016) Vertical distribution of photosynthetic nitrogen use efficiency and its response to nitrogen in field-grown maize. Crop Sci 56:397–407

Cirilo AG, Dardanelli J, Balzarini M, Andrade FH, Cantarero M, Luque S, Pedrol HM (2009) Morpho-physiological traits associated with maize crop adaptations to environments differing in nitrogen availability. Field Crops Res 113:116–124

Earl HJ, Tollenaar M (1999) Using chlorophyll fluorometry to compare photosynthetic performance of commercial maize (*Zea mays* L.) hybrids in the field. Field Crops Res 61:201–210

Evans J, Poorter H (2001) Photosynthetic acclimation of plants to growth irradiance: the relative importance of specific leaf area and nitrogen partitioning in maximizing carbon gain. Plant Cell Environ 24:755–767

Gallais A, Coque M (2005) Genetic variation and selection for nitrogen use efficiency in maize: a synthesis. Maydica 50(3/4):531–547

Gastal F, Lemaire G (2002) N uptake and distribution in crops: an agronomical and ecophysiological perspective. J Exp Bot 53:789–799

He P, Osaki M, Takebe M, Shinano T (2002) Changes of photosynthetic characteristics in relation to leaf senescence in two maize hybrids with different senescent appearance. Photosynthetica 40:547–552

Hidema J, Makino A, Mae T, Ojima K (1991) Photosynthetic characteristics of rice leaves aged under different irradiances from full expansion through senescence. Plant Phys 97:1287–1293

Hirel B, Martin A, Tercé-Laforgue T, Gonzalez-Moro MB, Estavillo JM (2005) Physiology of maize I: a comprehensive and integrated view of nitrogen metabolism in a C4 plant. Phys Plant 124:167–177

Kingston-Smith AH, Foyer CH (2000) Bundle sheath proteins are more sensitive to oxidative damage than those of the mesophyll in maize leaves exposed to paraquat or low temperatures. J Exp Bot 51:123–130

Kosgey JR, Moot DJ, Fletcher AL, McKenzie BA (2013) Dry matter accumulation and post-silking N economy of 'stay-green' maize (*Zea mays* L.) hybrids. Eur J Agron 51:43–52

Laemmli UK (1970) Most commonly used discontinuous buffer system for SDS electrophoresis. Nature 227:680–685

Makino A, Sakuma H, Sudo E, Mae T (2003) Differences between maize and rice in N-use efficiency for photosynthesis and protein allocation. Plant Cell Phys 44:952–956

Martinez DE, Costa ML, Gomez FM, Otegui MS, Guiamet JJ (2008) 'Senescence-associated vacuoles' are involved in the degradation of chloroplast proteins in tobacco leaves. Plant J 56:196–206

Masclaux-Daubresse C, Daniel-Vedele F, Dechorgnat J, Chardon F, Gaufichon L, Suzuki A (2010) Nitrogen uptake, assimilation and remobilization in plants, challenges for sustainable and productive agriculture. Ann Bot 105:1141–1157

Mu X, Chen Q, Chen F, Yuan L, Mi G (2016) Within-leaf nitrogen allocation in adaptation to low nitrogen supply in maize during grain-filling stage. Front Plant Sci 7:699

Osaki M (1995) Comparison of productivity between tropical and temperate maize: II. Parameters determining the productivity in relation to the amount of nitrogen absorbed. Soil Sci Plant Nutr 41:451–459

Paponov IA, Sambo P, Erley GSAM, Presterl T, Geiger HH, Engels C (2005) Grain yield and kernel weight of two maize genotypes differing in nitrogen use efficiency at various levels of nitrogen and carbohydrate availability during flowering and grain filling. Plant Soil 272:111–123

Ritchie SW, Hanway JJ, Thompson HE (1996) How a Corn plant develops. Special report, 48. Cooperative extension service. Iowa State University of Sciece and Technology, Ames

Rosenqvist E, van Kooten O (2003) Chlorophyll fluorescence: a general description and nomenclature. Practical applications of chlorophyll fluorescence in plant biology. Springer, New York, pp 31–77

Schippers JH, Schmidt R, Wagstaff C, Jing HC (2015) Living to die and dying to live: the survival strategy behind leaf senescence. Plant Phys. 169:914–930. http://www.trimble.com/Agriculture/greenseeker.aspx/. Accessed 13 Feb 2017 **(Trimble. Greenseeker crop sensing system)**

Thomas H, Ougham H, Canter P, Donnison I (2002) What stay-green mutants tell us about nitrogen remobilization in leaf senescence. J Exp Bot 53:801–808

van Oosterom EJ, Borrell AK, Chapman SC, Broad IJ, Hammer GL (2010) Functional dynamics of the nitrogen balance of sorghum, I. N demand of vegetative plant parts. Field Crops Res 115:19–28

Xiong D, Chen J, Yu T, Gao W, Ling X, Li Y, Peng S, Huang J (2015) SPAD-based leaf nitrogen estimation is impacted by environmental factors and crop leaf characteristics. Sci Rep 5:13389

Publisher's Note Springer Nature remains neutral with regard to jurisdictional claims in published maps and institutional affiliations.